ESCUELA TÉCNICA SUPERIOR DE INGENIEROS
INDUSTRIALES Y DE TELECOMUNICACIÓN

UNIVERSIDAD DE CANTABRIA

Trabajo Fin de Grado

Conversión fotoquímica de CO_2 a metanol en continuo en un sistema basado en un microreactor optofluídico

(Continuous photochemical conversion of CO_2 to methanol in an optofluidic microreactor)

Para acceder al Titulo de

Graduado/a en Ingeniería Química

Autor: Carlota Guati de Cabo

Escuela Técnica Superior de Ingenieros Industriales y de Telecomunicación

TÍTULO	**Conversión fotoquímica de CO_2 a metanol en continuo en un sistema basado en un microreactor optofluídico**		
AUTOR	**Carlota Guati de Cabo**		
DIRECTOR/CODIRECTOR	**Jonathan Albo Sánchez**		
TITULACIÓN	*Grado en Ingeniería Química*	FECHA	16/7/ 2018

PLABRAS CLAVE

Fotocatálisis; microreactor optofluídico; CO_2; dióxido de titanio.

PLANTEAMIENTO DEL PROBLEMA

La concentración del CO_2 en la atmosfera alcanza niveles récord cada año (411 ppm en mayo 2018) debido principalmente a la quema de combustibles fósiles. Se hace por tanto necesario, el desarrollo de procesos que permitan mitigar los impactos negativos de CO_2 en el clima, así como el desarrollo de nuevas fuentes de energía. La Captura y Utilización de CO_2 (CCU, por sus siglas en inglés) es una metodología con potencial para jugar un papel relevante en mantener el aumento de la temperatura de este siglo por debajo de los 2 grados centígrados (Acuerdo de París 2016). Existen diferentes vías para la conversión de CO_2, incluyendo la vía termodinámica, bioquímica, electroquímica o fotoquímica. La síntesis de productos útiles directamente bajo la luz solar es una tecnología prometedora para el almacenamiento de energía solar en forma de enlace químico, lo cual supone mitigar los efectos indeseables sobre el medio ambiente y al mismo tiempo, sintetizar productos útiles en condiciones ambientales. La fotoreducción de CO_2 puede resultar en diversos productos, incluyendo CO, HCOOH, alcoholes o hidrocarburos. Entre ellos, la síntesis de metanol es particularmente interesante, ya que puede ser utilizado como combustible o como producto intermedio en la síntesis de otros (e.j. tintes, resinas, adhesivos, etc.).

El objetivo de este trabajo es demostrar la conversión fotocatalítica de CO_2 a metanol en fase líquida y en continuo en un microreactor optofluídico. Los materiales seleccionados para la preparación de las superficies catalíticas son nanopartículas de óxido de titanio (IV) (TiO_2) y nanopartículas de óxido cuproso (Cu_2O). Se evalúan las variables de operaciones en el proceso para la conversión de CO_2: carga de material fotocatalítico en la superficie del fotoelectrodo, intensidad de la luz (UV y Vis), así como flujo de la disolución saturada de (0.5M $KHCO_3$) a la entrada de la celda.

RESULTADOS

Se ha determinado la productividad (r), como moles de metanol por hora y por área, y la efectividad cuántica aparente (AQY) del sistema, la cual compara el número de electrones que intervienen en la reducción de CO_2 con los generados en la superficie catalítica.

Para el caso de superficie catalítica formada únicamente por TiO_2 bajo irradiación ultravioleta, el mejor resultado se consiguió con las siguientes condiciones: 125 µl/min, 1mg/cm^2 and at 86 W/m^2 de caudal, carga catalítica e irradiancia, respectivamente. La productividad obtenida fue r=5x10^{-7} *MeOH* mol/cm^2·h y AQY=3.31%. Bajo luz visible no se detectó metanol. La metodología de Taguchi ha sido utilizada para determinar y verificar las mejores condiciones de operación, proporcionando un diseño de experimentos más rápido y eficaz.

Cuando la superficie catalítica estaba formada por Cu_2O/TiO_2 con un ratio en masa 50/50, la productividad obtenida bajo radiación ultravioleta fue r=2.23x10^{-6} *MeOH* mol/cm^2·h y AQY= 9.29%. Bajo luz visible los resultados fueron: r=9.4 x10^{-7} *MeOH* mol/cm^2 · h (AQY=3.95%). En este caso, las condiciones de operación fueron: 125 µl/min, 1mg/cm^2 y 130 W/m^2. Con el uso de nanopartículas de Cu_2O, tanto la productividad como la efectividad cuántica aparente han triplicado su valor respecto a los valores obtenidos con una superficie catalítica de TiO_2.

CONCLUSIONES

Se ha puesto en funcionamiento un microreactor optofluidico para la reducción de CO_2 de una forma exitosa. La utilización de este tipo de microreactor ofrece ventajas en términos de control de flujo, relación área volumen y transferencia de materia, mejorando respecto otros diseños como los reactores monolíticos.

Se han evaluado las diferentes condiciones de operación; caudal, carga catalítica e irradiancia, para maximizar la producción de metanol. En relación con el material catalizador, la adición de nanopartículas de Cu_2O ha mejorado los resultados obtenidos con superficies catalíticas de TiO_2. Esto se debe principalmente a que el óxido cuproso favorece la separación de cargas, evitando así efectos de recombinación de electrones. Además, su banda de conducción es más estrecha, centrándose en las reacciones de oxidación del H_2O y reducción del CO_2, así reacciones de no interés, como la reducción del H_2O, no se ven tan favorecidas. Futuros avances se centran en el desarrollo de nuevos materiales semiconductores, como las nanopartículas TiO_2/Cu *core-shell*, que por su morfología incrementarán la productividad del sistema.

BIBLIOGRAFÍA/REFERENCES

[1] Albo, J., et al. (2015). Green Chem. 17 (4), 2304-2324.

[2] Chen, R., et al. (2017). Chem. Eng. J. 316, 911–918.

Escuela Técnica Superior de Ingenieros Industriales y de Telecomunicación

TÍTULO	**Continuous photochemical conversion of CO_2 to methanol in an optofluidic microreactor**		
AUTOR	**Carlota Guati de Cabo**		
DIRECTOR/CODIRECTOR	**Jonathan Albo Sánchez**		
TITULACIÓN	*Grado en Ingeniería Química*	FECHA	16/7/ 2018

KEYWORDS

Photocatalyst; optofluidic microreactor; CO_2; titanium dioxide.

SCOPE

Every year a huge amount of fossil fuels is consumed to meet the rapid economic growth. Meanwhile, carbon dioxide (CO_2), the main greenhouse gas (GHG) source, is also emitted to the atmosphere. The global growth rate of atmospheric CO_2 has risen from 0.6 ppm per year in the early 1960s to an average of 2.3 per year during the past ten years, being the actual CO_2 concentration of 411 ppm. Carbon Capture and Utilization (CCU) has been proposed as a potential technological solution to the problems of GHG emissions and the growing energy consumption. CCU includes methods and technologies to remove CO_2 from flue gas streams and from the atmosphere, followed by recycling the CO_2 for future utilization through valuable products. The CO_2 conversion can be carried out by thermochemical, biochemical, electrochemical, photoelectrochemical, and photocatalytic processes. A promising way with increasing attention is the reduction of CO_2 by photocatalysis, which not only captures CO_2 but also simultaneously generates solar fuels under the sun. The photocatalytic reduction of CO_2 needs of multiple electron transfers, leading to the formation of different products. Although the studied process follows a complex chemical mechanism, with branching pathways giving different products, the production of methanol is particularly interesting. Methanol commonly uses are: reagent in several processes, fuel, solvent and biodiesel production.

The goal of this project is to characterize the continuous CO_2 photoconversion to methanol in liquid phase by using an optofluidic microreactor. The semiconductor materials used for the catalytic surfaces preparation are: titanium dioxide (TiO_2) and cuprous oxide (Cu_2O) nanoparticles. The following operation variables for the CO_2 reduction will be evaluated: 0.5M $KHCO_3$ inlet flowrate, catalytic load and irradiance (UV and VIS).

RESULTS

Productivity (r), defined as the moles of methanol generated in one hour per unit of active area, and Apparent Quantum Yield (AQY), that compares the electrons used in the reduction of CO_2 to methanol with the ones that are promoted from the catalytic surface, are determined in every set of experiments.

For the case of TiO_2 nanoparticles catalytic surface under UV irradiation, the best results were obtained at: 125 µl/min, 1mg/cm^2 and at 86 W/m^2 of flowrate, catalytic load and irradiance, respectively. Productivity was r=5x10^{-7} *MeOH* mol/cm^2·h and the AQY=3.31%. Under VIS irradiation, no methanol was detected by the Gas Chromatograph. Taguchi methods were also used in order to verify the best operation conditions of the system, providing a faster and a more effective design of experiments (DOE). When the catalytic surface was made of Cu_2O/TiO_2 with 50/50 weight ratio, productivity obtained under UV irradiation was r=2.23x10^{-6} *MeOH* mol/cm^2·h and the AQY= 9.29%. Under VIS irradiation, the results are: r=9.4 x10^{-7} *MeOH* mol/cm^2·h (AQY=3.95%). For this case, the operation variables were: 125 µl/min, 1mg/cm^2 y 130 W/m^2. By adding Cu_2O nanoparticles to the catalytic surface, Productivity and Apparent Quantum Yield were improved three times under UV irradiation regarding the use of only TiO_2 nanoparticles.

CONCLUSIONS

In this study, an optofuidic micoreactor-based experimental setup has been tested for the continuous photoreduction of CO_2 to methanol. It can provide a promising solution for the CO_2 challenge. Optofluidic microreactors present advantages from previous designs. The principal improvements are fine flow control, large surface-area-to-volume ratio and enhanced mass transfer. To maximize the methanol production, operation variables have been evaluated. Regarding the catalytic material, adding Cu_2O nanoparticles has improved the system performance. It is due to Cu_2O promotes charge separation, avoiding electron recombination effects on the catalytic surface. Moreover, its band gap is narrower than TiO_2; it also covers CO_2 reduction and H_2O oxidation reactions potentials. A smaller bandgap does not waste energy in non-interest reactions, such as water reduction. Future approaches focus on the development of new semiconductor materials, such as TiO_2/Cu *core-shell* nanoparticles. These nanoparticles will improve the system performance due to its morphology.

REFERENCES

[1] Albo, J., et al. (2015). Green Chem. 17 (4), 2304-2324.

[2] Chen, R., et al. (2017). Chem. Eng. J. 316, 911–918.

ACKNOWLEDGMENT

I would like to express my sincere gratitude to my project director, Jonathan Albo Sanchez, for his work, help and time in the development of this study. In addition, I would like to mention the opportunity that Ángel Irabien and the Department of Chemical and Biomolecular Engineering of University of Cantabria gave me when I decided to carry out this work. They also offered me the option to still working in this research during the summer.

I am also grateful to my fellows in the laboratory, for their help and the great moments we have spent together.

Finally, I also would like to mention my family and friends for their support during these four years and especially for the last months. They made the few free moments very enjoyable.

TABLE OF CONTENTS

A. LIST OF FIGURES ..... - iii -
B. LIST OF TABLES ..... - v -

1. INTRODUCTION ..... - 2 -

1.1. CO_2 challenge ..... - 2 -

1.2 Carbon Capture and Utilization (CCU) ..... - 3 -

1.3 Photocatalytic reduction of CO_2 ..... - 4 -

1.4 Background ..... - 8 -

1.4.1 Photoreactors ..... - 8 -

1.4.2 Photoactive electrode materials ..... - 9 -

A. Titanium Dioxide ..... - 9 -

B. Cuprous Oxide ..... - 10 -

2. OBJECTIVES ..... - 11 -

3. METHODOLOGY ..... - 12 -

3.1. Description and dimensions of optofluidic microreactor ..... - 12 -

3.1.1. General description ..... - 12 -

3.1.2. Elements and detailed dimensions ..... - 13 -

3.2 Equipment and configuration ..... - 14 -

3.3 Experimental procedure ..... - 15 -

3.3.1 Photoactive surfaces preparation ..... - 15 -

3.3.2. Guidelines ..... - 16 -

3.4. Experimental Data Analysis ..... - 17 -

3.4.1. Productivity and Apparent Quantum Yield ..... - 17 -

3.4.2. Taguchi Methods ..... - 19 -

4. RESULTS ..... - 20 -

4.1. Activity with time ..... - 20 -

4.2 Operation Conditions for TiO_2-based surfaces ..... - 21 -

A. Effect of the liquid flowrate ..... - 21 -

B. Effect of the light intensity ..... - 22 -

C. Effect of TiO_2 loading. ..... - 23 -

4.3 Taguchi and best operation conditions. ..... - 24 -

4.4 Comparison of TiO_2 /Cu_2O under UV-light and visible light. ..... - 27 -

5. CONCLUSIONS ..... - 29 -

6.CHALLENGES AND PERSPECTIVES ..... - 31 -

7. REFERENCES ..... - 32 -

8. ANNEX ..... - 35 -

8.1 Characterization of the pilot plant set up ..... - 35 -

8.2 LED Characterization regarding distance to the catalytic surface ..... - 36 -

8.3 Calibration lines for the studied compounds. ..... - 37 -

LIST OF FIGURES

Figure 1. CO_2 concentration in the atmosphere from 2012-2016. Monthly Average in Mauna Loa Observatory (Hawaii). Figure from ref [3]……2

Figure 2. Carbon Capture Utilization Scheme. Figure from ref [7]……4

Figure 3. Photoinduced formation of an electron–hole pair in a semi- conductor with possible decay paths. Figure from ref [12]……6

Figure 4. Conduction band, valence band potentials, and band gap energies of various semiconductor photocatalysts relative to the redox potentials at pH 7 of compounds involved in CO_2 reduction. Figure from ref [4]……7

Figure 5. Schematic of TiO_2 photocatalyzed reaction where CB and VB represent the conduction band, and valence band, respectively. Figure from ref [23]……10

Figure 6a. Absorption spectra of the two-catalyst used in the study. Sigma Aldrich TiO_2, nanopowder 21 nm. Figure from ref [27]……11

Figure 6b. Absorption spectra of the two-catalyst used in the study. UV–Vis DR spectra of the Titanium Dioxide NanoTube arrays (TNTs) and Cu_2O/TNTs with different electrodeposition charges. Figure from ref [25]……11

Figure 7a. Optofluidic microreactor. Inner part of the optofluidic microreactor……13

Figure 7b. Optofluidic microreactor. Staging of the microreactor working with UV light at 5 cm from the electrode surface……13

Figure 8. Optofluidic microreactor assembly……14

Figure 9a. Lab scale pilot plant for the continuous photoreduction of CO_2 with LED technology……15

Figure 9b. Scheme of the set up……15

Figure 10. Harder & Steenbeck Airbrush……16

Figure 11. TiO_2 nanoparticles (21 nm) based surfaces at loadings ranging from 0.5 mg/cm^2 to 3.0 mg/cm^2……16

Figure 12. Catalytic TiO_2 nanoparticle activity determination. 1mg/cm^2 electrode at 109 µL/min and at 130 W/m^2……20

Figure 13. Effect of the liquid flowrate on methanol productivity and AQY for an 1mg/cm^2 electrode at 86 W/m^2……21

Figure 14. Effect of the irradiance on methanol productivity and AQY for a 2 mg/cm^2 electrode at 109 µl/min……22

Figure 15. Effect of the electrode load on methanol productivity and AQY at 86 W/m^2 and a flowrate of 109 µl/min……23

Figure 16. Main effect plot for methanol productivity means……26

Figure 17. Main effect plot for Signal-to-Noise ratios……26

Figure 18a. Cu_20/TiO_2 50/50 weight ratio electrode before being used……27

Figure 18b. Cu_20/TiO_2 50/50 weight ratio electrode after the first used. Oxidation phenomena……27

Figure 19. Use effect in Cu_2O/TiO_2 50/50 weight ratio electrode……28

Figure 20. Effect of Cu_2O addition into the TiO_2 catalytic surface. 50/50 weight ratio electrode……28

Figure A1a. Typical relative spectral power vs. wavelength at 25°C for 365nm UV LED Gen2 Emitter LED ENTER……35

Figure A1b Typical relative spectral power vs. wavelength at 25°C for High Luminous Efficacy Cool White LED Emitter LED ENTER……35

Figure A2 Calibration curve for inlet flowrate controlled by Peristaltic Pump Miniplus 3 Gilson……35

Figure A3 Irradiance of UV LED at difference distance from the electrode surface: 2; 5 and 8.5cm……36

Figure A4 Irradiance of visible light LED at difference distance from the electrode surface: 2; 3.5; 5 and 8.5cm……36

Figure A5 Calibration curve for methanol concentration detected by Gas chromatograph (GCMS-QP2010 Ultra Shimadzu)……37

Figure A6 Calibration curve for isopropanol concentration detected by Gas chromatograph (GCMS-QP2010 Ultra Shimadzu)……..37

Figure A7 Calibration curve for formic acid concentration detected by Ion Chromatography (IC)……38

LIST OF TABLES

Table 1. Characterization of the feed solution at 25℃ and 101.3 kPa CO_2 partial pressure. Table from ref [15]……..8

Table 2. Three-Level Orthogonal Array L9 Standard and results……..25

ABSTRACT

Among the different alternatives to reduce CO_2 emissions, Carbon Capture and Utilization (CCU) is particularly an interesting approach since it allows to reduce the reliance on fossil fuels and produce, at the same time, value added chemicals. This study shows how the photocatalytic reduction of CO_2 may represent a suitable technology for tackling the CO_2 challenge. By using an optofluidic microcell and TiO_2 and Cu_2O/TIO_2 as photoactive surfaces, is possible to continuously convert CO_2 to methanol with a maximum production rate and apparent quantum yield under UV irradiation of r= $2.23x10^{-6}$ *MeOH mol/cm²h* and *AQY*= 9.29% at 125 µl/min, 1mg/cm2 and at 86 W/m² of flowrate, catalytic load and irradiance, respectively for a Cu_2O-based photoactive surface. The optofluidic microreactor reported in this study has shown some advantages from previous designs, such as fine flow control, large surface-area-to-volume ratio and enhancement of mass transfer and microreactor illumination. The research efforts carried out are a step forward into the development of innovative processes for the continuous CO_2-to-methanol reaction.

1. INTRODUCTION

1.1. CO_2 challenge

Every year a huge amount of fossil fuels is consumed to meet the rapid economic growth. Meanwhile, carbon dioxide (CO_2), the main greenhouse gas (GHG) source, is also emitted to the atmosphere. CO_2 accounts for approximately 70% of the GHG radiative forcing from among the other main GHGs (CH_4, N_2O, CF_4, C_2F_6, SF_6). Thus, it makes sense to focus on the reduction of CO_2 net emissions by any mean [1]. Rising atmospheric levels of this chemical compound and the depletion of fossil fuel reserves are becoming serious concerns due to its impact in the environment and socio-economic aspects of life. The global growth rate of atmospheric CO_2 has risen from 0.6 ± 0.1 ppm per year in the early 1960s to an average of 2.3 ± 0.6 ppm per year during the past ten years, being the actual CO_2 concentration of 411 ppm [2]. ***Fig. 1*** shows the exponential CO_2 concentration tendency along time. This is a clear evidence that Paris Climate Agreement (March 2016) is not going to be achieved easily.

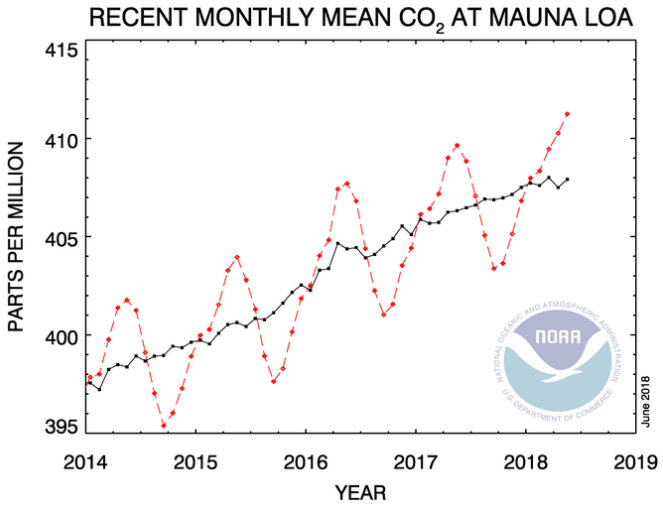

Figure 1. CO_2 concentration in the atmosphere from 2012-2016. Monthly Average in Mauna Loa Observatory (Hawaii) [3].

The Paris Agreement contains a long-term temperature goal of keeping the increase in the global average temperature below 2°C and pursuing efforts to limit this increase to 1.5°C above preindustrial levels. The Paris Agreement also contains long-term global emissions goals to peak these emissions as soon as possible and then reduce them

rapidly, according to the best available science and techniques. This goal requires introducing negative CO_2 emissions at a small scale.

Given the current economic and political, it is natural to seek for ways other than storage by which mankind can decrease GHG emissions. Anthropogenic activities actually generate 37 Gt of CO_2 emissions, this contribution will increase up to 38-46 Gt by 2019 depending on the policies each country adopt and even if renewable sources becomes the first energy supply [4]. To simultaneously reduce the high CO_2 emissions and the depletion of fuels, the conversion of GHG gas into useful fuels or other valuable products has become an important solution for sustainable energy and environmental development.

This way of thinking belongs to what is called '*circular economy*'. This development model turns products that are at the end of their service life into resources for others, closing loops in industrial applications and minimizing waste. A study of seven European nations found that a displacement to a circular economy model would reduce each nation's GHG emissions by up to 70% and grow its workforce by about 4% [5].

1.2 Carbon Capture and Utilization (CCU)

In recent years, carbon capture and utilization (CCU) has been proposed as a potential technological solution to the problems of GHG emissions and the growing energy consumption. CCU includes methods and technologies to remove CO_2 from flue gas streams and from the atmosphere, followed by recycling the CO_2 for future utilization through valuable products.

Despite the adoption of alternative energy sources and energy efficient systems to reduce the rate of CO_2 emissions, the cumulative amount of CO_2 in the atmosphere needs to be reduced to limit the negative impacts of climate change [6].

The utilization of CO_2 as a feedstock to make valuable chemicals, materials, and transportation fuels is potentially more desirable and provides a better and long-term solution than storage. The products of CO_2 utilization can supplement or replace chemical feedstocks in the fine chemicals, pharmaceutical, and polymer industries.

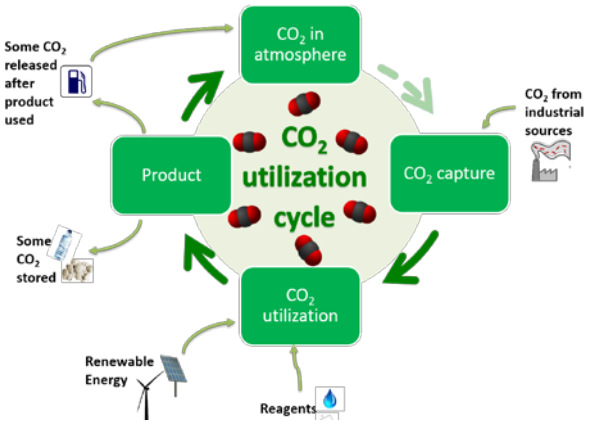

Figure.2 Carbon Capture Utilization scheme. [7]

The CO_2 conversion can be carried out by thermochemical, biochemical, electrochemical, photoelectrochemical, and photocatalytic processes. Electrochemical reduction is well known to produce a variety of useful products, such as carbon monoxide, formic acid, formaldehyde, methanol, oxalic acid, etc. But it is still far from the green development concept due to it depends on any electric energy source. In case of biochemical conversions, aquacultures of microalgae are frontrunners for photosynthetic capture of CO_2 from flue gases. On the other hand, thermochemical conversions, have smaller carbon and energy losses but yield a mixture of products [8].

1.3 Photocatalytic reduction of CO_2

A promising way with increasing attention is the reduction of CO_2 by photocatalysis, which not only captures CO_2 but also simultaneously generates solar fuels under the sun. The photocatalytic reduction of CO_2 represents an environmentally friendly and economical solution for the CO_2 challenge. The required catalyst materials, semiconductors or transition-metal complexes are usually abundant and low-cost. The photocatalytic reduction of CO_2 needs of multiple electron transfers, leading to the formation of different products. Depending on the specific reaction pathway taken place during the process and the number of electrons transferred, the most common products are: carbon monoxide, formic acid, formaldehyde, methanol, methane, ethane, and ethene [9]. Although the studied process follows a complex chemical mechanism, with branching pathways giving different products, the production of methanol is particularly interesting.

Methanol commonly uses are: reagent in several processes, fuel, solvent and biodiesel production. Although in Europe it is not a product very demanded, in South America and Asia Pacific (APAC), prices are likely to witness a gradual increase due to strong demand. One of the main advantages of methanol production by photocatalytic reduction of CO_2 is that it can be performed under ambient conditions. This process is becoming feasible and renewable at human timescale [10].

In the next five years, the global demand for methanol is expected to grow at an average rate just over 5%, but its demand for fuel applications is expected to rise more strongly at a rate of about 6.5% [11]. Compared to hydrogen, it possesses a higher energy density and it can be stored at atmospheric pressure.

The photocatalytic conversion of CO_2 makes use of semiconductors to promote reactions in the presence of light irradiation. They are an attractive type of material because of their energy **band gap**[1]. The process of photochemical reduction of CO_2 is also known as artificial photosynthesis. The mechanism can be summarized in three steps [4]:

- Generation of charge carriers (electron–hole pairs) upon absorption of photons with suitable energy from light irradiation.
- Charge carrier separation and transportation.
- Chemical reactions between surface species and charge carriers.

Upon absorption of a photon with energy equal to or higher than the **band gap**, an electron is excited from the valence band (VB) to the conduction band (CB), thus it leaves an empty state that constitutes a quasiparticle that is referred to as a hole. Alternatively, these electrons can travel to the surface of the semiconductor and react with surface adsorbed species (CO_2 in this case). Electrons in the CB reduce CO_2, whereas holes in the VB oxidize water to oxygen.

[1] **Band gap**: distance between the valence band of electrons and the conduction band. Essentially, the band gap represents the minimum energy that is required to excite an electron up to a state in the conduction band where it can participate in conduction

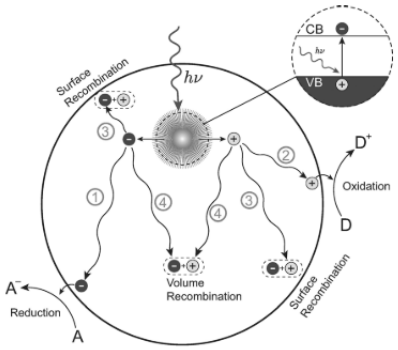

Figure.3 Photoinduced formation of an electron–hole pair in a semi- conductor with possible decay paths. A=electron acceptor, D=electron donor [12].

In order to reduce CO_2 to methanol, electrons in the semiconductor are required to have more negative chemical potential than the potential for methanol formation. Water oxidation takes part at the same time. The energy provides by the excitation of negative charge from the semiconductor make the system below spontaneous. Because formic can be an intermediate in the formation of methanol, its reduction potential is also included [13].

- $2H_2O \rightarrow O_2 + 4\,H^+ + 4\,e^-$ $\quad \varepsilon \circ = +0.81eV \quad pH = 7$
- $CO_2 + 6\,H^+ + 6\,e^- \rightarrow CH_3OH + H_2O$ $\quad \varepsilon \circ = -0.38\,eV \quad pH = 7$
- $CO_2 + 2\,H^+ + 2\,e^- \rightarrow HCOOH$ $\quad \varepsilon \circ = -0.61\,eV \quad pH = 7$

Fig.4 represents the electrochemical potential compared to the normal hydrogen electrode (NHE) of common semiconductors materials. In the case of TiO_2, its band gap is a wide range (3.2 - 3.0 eV), more details are given in **1.4.2 Photoactive electrode materials**. Besides reduction of CO_2 to methanol, ***Fig.4*** also includes the potential to formic acid and formaldehyde, as possible intermediates in the production of methanol.

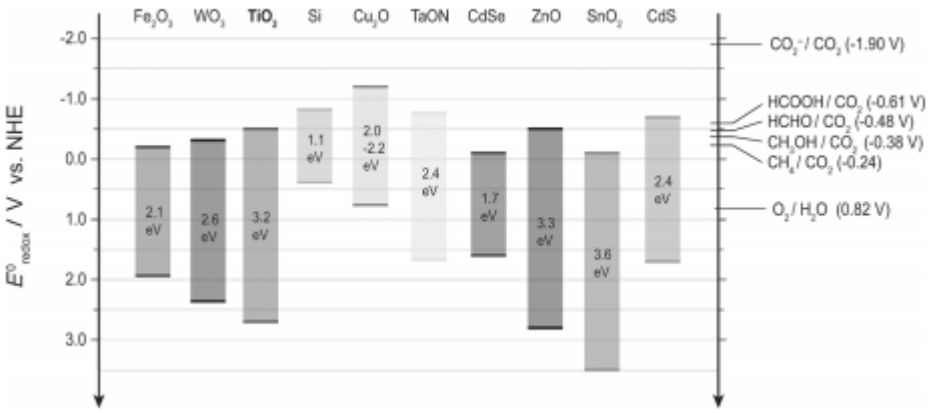

Figure.4 Conduction band, valence band potentials, and band gap energies of various semi-conductor photocatalysts relative to the redox potentials at pH 7 of compounds involved in CO_2 reduction [4].

Water acts as electron donor. However, reduction of water to H_2 could also take part instead of reduction of CO_2. It is crucial to suppress the concurrent generation of hydrogen, which competes with carbon species for the generated electrons. Moreover, surface adsorption of H_2O is preferable over CO_2 in the liquid phase, and thus the reduction of water is favorable.

Reactions below represent reduction potential for water and CO_2, their values are very similar, which makes this competition an issue to consider.

- $2H_2O + 2\,e^- \rightarrow H_2 + 2OH^-$ $\qquad \varepsilon \circ = -0.41eV \qquad pH = 7$
- $CO_2 + 6\,H^+ + 6\,e^- \rightarrow CH_3OH + H_2O$ $\qquad \varepsilon \circ = -0.38\,eV \qquad pH = 7$

The reaction selectivity can be controlled by the photocatalyst material applied, photocatalysts' morphology, changing the exposed facets and introducing new reaction sides and doping materials. Knowing the mechanism may enable an increase in the overall conversion of CO_2 through minimization of thermodynamics and kinetics barriers. Using $KHCO_3$ buffer solutions may involve these possible reactions for methanol formation. All data correspond with $pH = 7$:

- $H_2CO_3 + 6\,H^+ + 6\,e^- \rightarrow CH_3OH + 2H_2O \qquad \varepsilon \circ = +0.044\,eV$
- $HCO_3^- + 7\,H^+ + 6\,e^- \rightarrow CH_3OH + 2H_2O \qquad \varepsilon \circ = +0.044\,eV$
- $CO_3^{2-} + 8\,H^+ + 6\,e^- \rightarrow CH_3OH + 2H_2O \qquad \varepsilon \circ = +0.209\,eV$

In water, when a bicarbonate concentration is below its saturation concentration, the bicarbonate salt dissociates. Considering $KHCO_3$ solubility is 33.7g /L at 20 C [14], it can

be assumed that all the salt is dissociated in water. This assumption was taken by *N Gupta et al.* in their study about $KHCO_3$ equilibrium in presence of CO_2 gas phase at different initial concentrations [15].

The table below show the characterization of the feed, this information could be used as a first attempt to understand the reaction mechanisms inside the cell. However, due to the complexity of the photochemical system, the comprehension of the chemical mechanism is still far from being understood. Modeling of the kinetics of the microcell is not trivial [16].

Table.1 Characterization of the feed solution at 25°C and 101.3 kPa CO_2 partial pressure. [15]

Electrolyte concentration (M)	***CO_2 (aq) (M)***	***HCO_3^- (aq) (M)***	***CO_3^{2-} (aq) (M)***	***pH***
0.5	0.0342	0.499	$7.4 \cdot 10^{-4}$	7.5

The influence of the pH can be explained with respect to species present in which case. At pH= 8, the CO_2 dissolved is present as CO_2/HCO_3^-, in pH= 9 the CO_2 is almost equally divided between the HCO_3^-/ CO_3^{2-} species and in pH= 10 there are more CO_3^{2-} species than HCO_3^- species, and in pH 11 the predominance is almost totally of CO_3^{2-} species [17]. This leads to different concentrations of species at different values of pH. Species and anions produced by the theoretical reduction of H_2CO_3 and carbonate ions, act also as precursors for the additional formation of methanol. Data are referred to $pH = 7$.

- $H_2CO_3 + 2\,H^+ + 2\,e^- \rightarrow HCOOH + H_2O \qquad \varepsilon \circ = -0.166\,eV$
- $HCOO^- + 5H^+ + 4\,e^- \rightarrow CH_3OH + H_2O \qquad \varepsilon \circ = +0.157\,eV$

1.4 Background

1.4.1 Photoreactors

The reactor design is an important factor that highly affects the performance of the photosystem. Photoreactor development is an engineering approach to enhance efficiency of CO_2 reduction. The UV and visible light reactor systems can be grouped into two main categories: fluidized bed reactor and fixed bed reactor. Fluidized bed reactor, also known as slurry reactor, is operated as a batch process in two-phase heterogeneous

system. Such types of reactor design face various problems such as presence of fine solid phase catalyst which led to fouling of radiation source, less active surface contact area, and additional cost during the separation of fine catalyst particles.

Wu et al. also developed fiber reactor, a type of fixed bed reactors, to reduce the loss of light. Quantum efficiency (0.049%) achieved in the optical fiber reactor is higher than that in a conventional batch reactor (0.002%) [16].

The synergy of microfluidics and optics, what is called optofluidics, has been recently applied to photoreactor design, showing a better performance than previous designs. It has been reported that microreactors can be classified in several categories, such as micro-capillary, single microchannel, multi-microchannel and planar microreactors, [18].

Optofluidic microcell is a planar microreactor that presents advantages from previous designs (i.e. slurry reactor, fiber reactors and monolith reactors). The principal improvements are: fine flow control, large surface-area-to-volume ratio and enhanced mass transfer [19]. The incorporation of optofluidic into the photoreactor design can greatly reduce the requirements for time, sample volume and equipment. Besides this, working in a continuous system represents advantages in the face of batch systems, since it could be coupled to CO_2 emission points.

Xiao Cheng et al have previously worked with an optofluidic microreactor. Their photocatalytic reactor improved the performance for the photocatalytic conversion of CO_2, reaching a methanol formation rated of 454.6 mmol/g-cat·h. [20]. In comparison to common photocatalytic cell configurations, such as the optical-fiber photo reactor, the methanol yield has already been improved in five orders of magnitude. Some studies show a methanol yield of 0.02 μmol/g-cat·h using optical-fiber photo reactor comprised of near 120 Cu/TiO_2-coated fiber [21].

1.4.2 Photoactive electrode materials

A. Titanium Dioxide

TiO_2 is the most investigated photocatalyst for artificial photosynthesis due to its excellent chemical and physical properties. Besides these features, this material provides high oxidation efficiency, nontoxicity, high photostability and chemical

inertness. Pure TiO_2 has some serious disadvantages that restrict its wide applications [22]. For this reason, it is promoted the use of mesoporous materials and structures with large specific surface area and pore volume. In case of TiO_2 nanoparticles, a higher surface area can be achieved. It makes TiO_2 a good nanomaterial for the manufacture of several catalysts that enhance reductive activity. The phase structure and surface properties of this oxide have a strong influence on the final performance. It has been studied that anatase structure provides better efficiencies under UV irradiation than rutile because of the number of a higher atoms exposed per face [22]. Nano TiO_2 particles has been proved to be one of the most active photocatalytic semiconductor under ultraviolet radiation.

Coming back to photoreduction mechanism TiO_2 presents a very suitable band gap that allows the reduction of CO_2 and the oxidation of water at the same time.

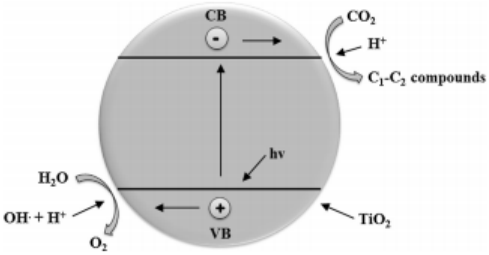

Figure.5 Schematic of TiO_2 photocatalyzed reaction where CB and VB represent the conduction band, and valence band, respectively.[23]

For an H_2O electron to be donated to the vacant hole, the redox potential level of the donor is thermodynamically required to be above the VB position of the TiO_2 material (*+2.8 eV*), while that of the acceptor should be below the CB position (*-0.5 eV*). CO_2 reduction and H_2O oxidation meet these requirements. TiO_2 bandgap depends on the morphology, being TiO_2 3.2 eV for anatase, 3.0 eV for rutile and 3.4 eV for brookite.

B. Cuprous Oxide

Cu_2O is a cheap, relatively abundant and intrinsically p-type[2] semiconductor with a low bandgap of about 2 - 2.2 eV. ***Fig.4*** compares band gaps from different materials. In

[2] As opposed to *n-type* semiconductors, *p-type* semiconductors have a larger hole concentration than electron concentration. In *p-type* semiconductors, holes are the majority carriers and electrons are the minority carriers.

theory, the narrow bandgap and appropriate positioning of the conduction and valence make Cu_2O an ideal photocatalyst for CO_2 reduction [24]. The same as TiO_2, Cu_2O exposed facets have been reported to have an important role in CO_2 reduction. It was recently found that Cu_2O is an appropriate candidate photocatalyst for CO_2 photoreduction driven by visible light [4].

Cu_2O matches well with the relevant sunlight spectrum and a conduction band that is more negative than that of TiO_2. Thus, when TiO_2 is combined with Cu_2O, the photoexcited electrons would transfer from the conduction band of Cu_2O to that of TiO_2 and subsequently initiate a photoreduction reaction [16]. More recently, a Cu_2O/TiO_2 heterostructure has been reported for CO_2 photoreduction showing enhanced photocatalytic activity compared to the pure TiO_2 under the UV illumination [25].

Besides the material features related to the chemical potential, other important aspect to consider is their optical absorption range. As it can be observed from ***Fig.6*** TiO_2 could shift its optical absorption edge from UV to visible light range by doping it with Cu_2O. Since visible light accounts for 45% of the solar spectrum [26], there is a need to develop titanium based photocatalysts which are active under the visible light spectrum.

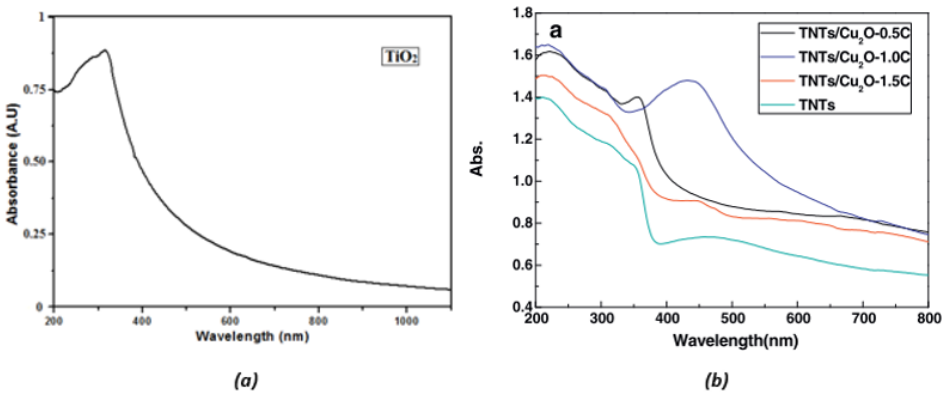

Figure.6 Absorption spectra of the two-catalyst used in the study. **(a)** Sigma Aldrich TiO2, nanopowder 21 nm [27] **(b)** UV–Vis DR spectra of the Titanium dioxide NanoTube arrays (***TNTs***) and Cu2O/TNTs with different electrodeposition charges [25].

2. OBJECTIVES

As a result of all the concerns related to CO_2 emissions and depletion of fossil fuels, the main purpose of this study is to enhance methanol yield from the continuous photoreduction of CO_2 in an optofluidic microreactor, making CO_2 utilization a feasible option for a more sustainable future.

Accordingly, the objectives of the present project are as follows:

- To set-up a lab scale experimental plant based on an optofluidic microreactor for CO_2 photoreduction.
- To prepare photoactive surfaces based on TiO_2 nanoparticles and TiO_2 doped with Cu_2O.
- To evaluate the key operation variables in the continuous CO_2 photoreduction process: flowrate, catalyst loading, light type (UV/Vis) and intensity.
- To analyse the methanol production rates and efficiencies and predict optimal operation conditions with a Taguchi method.

3. METHODOLOGY

3.1. Description and dimensions of optofluidic microreactor

3.1.1. General description

As shown in ***Fig.7***, the microcell contains two microchambers, separated by an impermeable polymer barrier where the photoactive surface is placed. Light strikes directly on the catalytic surface and liquid flows through it, allowing the reaction to take place.

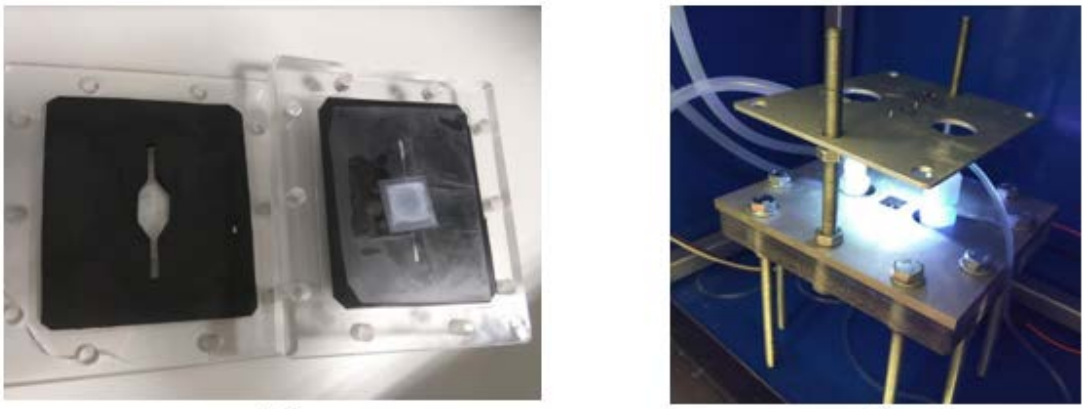

Figure.7 Optofluidic microcell. **(a)** Inner part of the optofluidic microcell **(b)** Staging of the microcell working with UV light.

3.1.2. Elements and detailed dimensions

The microreactor consists of two rectangular compartments of *Poly-methyl methacrylate* (PMMA) which provides an uniform light distribution. The microchamber shape was designed in such a manner to promote the well distribution of the fluid inside the microcell. The photon receiving area is 1 cm^2. The LEDs used (UV, 365-370nm, and VIS, 450 nm) are low power performance for avoiding overheating on the catalytic surface. Temperature on the catalytic surface was measured with an infrared thermometer. LEDs are hold by two screws on both sides of the main body, so distance to the catalytic surface can be regulated with washers.

A stainless-steel plate was included on the top to homogeneously distribute the pressure over the entire surface, avoiding stress in the screw points and possible fractures.

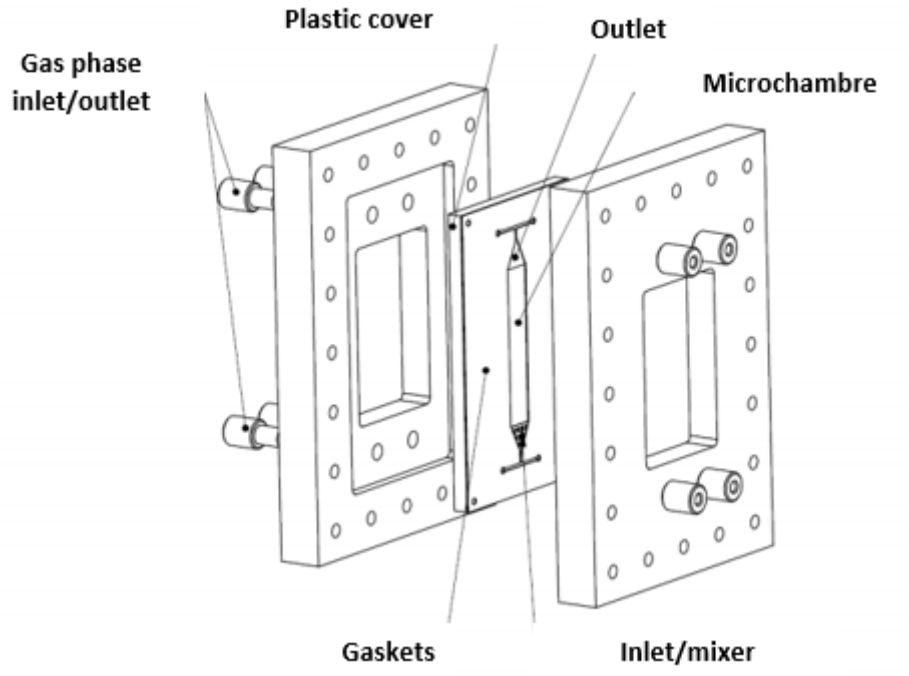

Figure.8 Optofluidic microreactor assembly.

3.2 Equipment and configuration

The system is equipped with the following elements. ***Fig.9*** shows a schematic representation of the plant configuration:

- Peristaltic Pump Miniplus 3 Gilson
- Power control panel
- Feed stirred tank
- Dark box, where the microcell is located.

Besides the equipment involved in the plant, there are other main parts needed for the experimental procedure: *Harder & Steenbeck airbrush* and *Ultrasonic H-D Selecta P* for the ink preparation. For irradiance measurements, a radiometer is used (*Photoradiometer Delta OHM HD 2102.1*).

Gas chromatograph (GCMS-QP2010 Ultra Shimadzu) equipped with a Flame Ionization Detector (FID) for the methanol detection. The chromatograph uses Helium as a carrier gas at a flow rate of 50 ml min^{-1}. For formic acid detection, an *ion chromatography (IC)*, Dionex ICS-1100, with an IonPac AS9-HC Analytical column (4-mm) was used. The

column is made of supermacroporous polyvinylbenzyl ammonium polymer cross-linked with divinylbenzene. The mobile phase is a 4.5 mM solution of sodium carbonate.

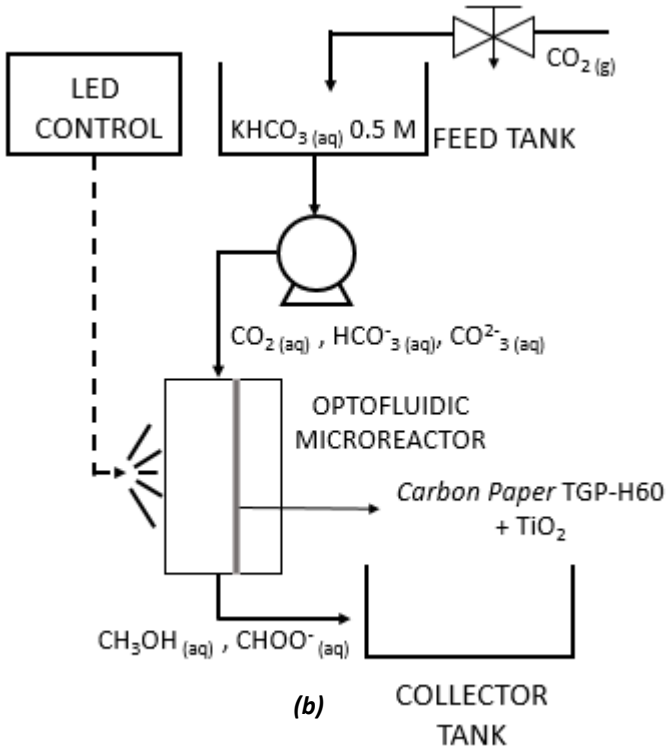

(a) ***(b)***

Figure.9 **(a).** Lab scale plant for the continuous photoreduction of CO_2 with LED technology. **(b)** Scheme of the set up

3.3 Experimental procedure

3.3.1 Photoactive surfaces preparation

The electrodes, whose total area is 2.25 cm^2, were manufactured by airbrushing a catalytic ink onto a porous carbon paper type TGP-H60 (Toray Inc.). Once the electrode is located inside the microcell, the available area is 1 cm^2. This catalytic ink was formed by a mixture of the selected particles (Sigma Aldrich TiO_2, nanopowder 21 nm primary particle size, 99.5% purity or/and Copper(I) oxide, 97%, ACROS Organics™) as electrocatalyst, Nafion® dispersion 5 wt.% (Alfa Aesar) as binder and isopropanol (IPA) (Sigma Aldrich) as vehicle, with a 70/30 catalyst/Nafion mass ratio and a 3% solids (semiconductor + Nafion) percentage; this mixture was sonicated for 30 min at ambient temperature [28]. When Cu_2O nanoparticles were used, weight ratio of Cu_2O/ TiO_2 was 50/50.

Figure.10 Harder & Steenbeck airbrush

Semiconductor loading was controlled by continuous weights during the airbrushing process. While catalytic ink was distributed on the electrode surface, 110℃ was applied, so the IPA was vaporized. All electrodes were dried at ambient conditions for 2h and then kept in plastic bags for preventing them from being humidified in an open atmosphere.

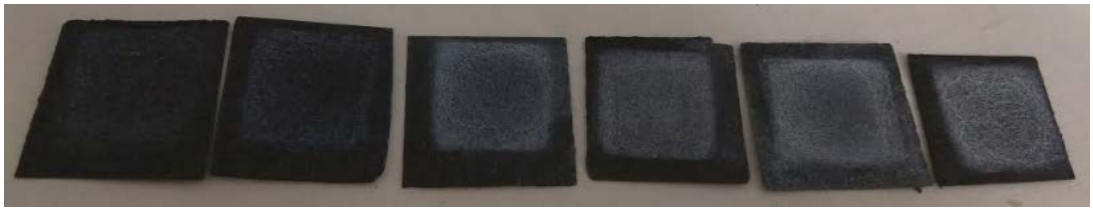

Figure.11 TiO_2 nanoparticles (21 nm) based surfaces at loadings ranging from 0.5 mg/cm^2 to 3.0 mg/cm^2.

3.3.2. Guidelines

CO_2 saturated solution: A 0.5M $KHCO_3$ (*AppliChem Panreac ITW Companies*) solution is saturated with CO_2 during 20 min. Limited solubility of CO_2 in water is one the crucial problem to drive photocatalytic reduction of CO_2 efficiently. The solubility of CO_2 in water can be improved by using $KHCO_3$, as discussed before. This saturated solution is pumped by the peristaltic pump to the inlet of the optofluidic microreactor.

Pattern solutions: methanol, ethanol, isopropanol and formic acid curves were obtained in the range of 1 to 50 ppm in $KHCO_{3\,(aq)}$ CO_2 saturated solution. The lines are included in the Annexes. These lines allow determining the final product concentration.

Calibration lines for liquid flow and light intensity: Flowrate is controlled with pump rpm and irradiance with the LED distance to the active surface and the power of the control panel. Calibration lines are included in Annexes.

Staging of the optofluidic microcell: This step involves the positioning of the electrode inside the cell, closing the cell by adjusting ten screws, positioning the LED on the top of the microcell with a regulated distance, 5 cm, where enough light intensity is achieved. A range from 85 to 260 W/m^2 can be tested.

Connect the cell with the stirred feed tank and the tube collector. This is a key step because a little variation on how the cell is connected, it may modify the inner pressure making the fluid pass by the non-illuminated area.

Selection of variable ranges: Load and flowrate ranges and intensity were selected according to previous literature on the use of TiO2 photoactive surfaces [19, 29].

- Flowrate: 65, 85, 109, 125 and 165 µL/min.
- Intensity: 85, 130, 170, 210 and 260 W/m^2.
- Load: 0.5, 1.0, 2.0 and 2.5 mg/cm^2

Collecting samples: Each test tube is 10 ml volume. Two/three samples are collected when steady state is reached (productivity can be considered constant).

Analysis in GC: The samples are analyzed in ascending concentration order. Distilled water samples are also included for cleaning the column between different experiments. Patrons are also included in order to verify a correct measurement.

Analysis in the Ionic Chromatographs: The Thermo Scientific Dionex™ ICS-1100 Ion Chromatography System (Dionex ICS-1100) performs ion analyses using suppressed or non-suppressed conductivity detection. To perform the measurements, the mobile phase of 4.5 mM solution of sodium carbonate will be set as the zero in conductivity.

3.4. Experimental Data Analysis

The performance of the system was determined from the concentration of methanol within 90 minutes of irradiation, when the system seems to be stable. Those data that double the average or by contrast are below its half are not considering for calculations.

Experimental error was calculated as the standard deviation of three experiments, when possible. In most of the experiments, the error was within 10% in most of the cases and the reproducibility was satisfactory.

3.4.1. Productivity and Apparent Quantum Yield

Productivity is defined as the moles of methanol generated in one hour per unit of active area. This is an effective way of quantifying the performance of the system, allowing evaluating the rate of methanol production in different scenarios.

$$Productivity\ (P) = Conc.\ (mmol \cdot L^{-1}) \cdot Flowrate\ (L \cdot h^{-1}) \cdot Area^{-1}(m^{-2}) \qquad (1)$$

Apparent Quantum Yield (AQY) compares the electrons used in the reduction of CO_2 to methanol with the ones that are promoted from the valence band to the conduction band. This parameter assumes that per photon that strikes on the catalytic area one electron is promoted to the conduction band and can participate in the formation of methanol.

Firstly, the photon flux input should be determined according to:

$$Photon\ flux\ input = \frac{I_{int}(W \cdot m^{-2}) \cdot A\ (m^2) \cdot \lambda\ (m)}{h\ (J \cdot s) \cdot c\ (m \cdot s^{-1})} \qquad (2)$$

Where:

$I_{int} = Irradiency\ to\ the\ catalytic\ surface\ (W \cdot m^{-2})$

$A = Catalytic\ area\ exposured\ to\ light\ (m^2)$

$\lambda\ = Wavelenght\ (m)$

$h = Plank\ constant\ (J \cdot s)$

$c = Light\ velocity (m \cdot s^{-1})$

$$AQY(\%) = \frac{n_e \cdot N_A \cdot mol\ CH_3OH}{Photon\ flux\ input\ (s^{-1}) \cdot time\ (s)} \cdot 100 \qquad (3)$$

Where:

$n_e = Number\ of\ electrons\ needed\ in\ the\ reduction\ reaction\ (-)$

$N_A = Avogadro\ Number$

3.4.2. Taguchi Methods

The design of an experiment (DOE) is not a simple one-step process but is actually a series of steps that must follow a certain sequence for the experiment to yield improvement better understanding of the process performance [29]. Taguchi methods focus on the reduction and control of variability in a given process/product. In this case, Taguchi could be used for assuring methanol production will be more robust and the highest possible according to the system features. Although Taguchi method is actually performed in industries for product design and quality, its technique could be used as well in the research field. It also helps the first approach to a new process, where the interactions of the variables and how they will affect the result are unknown. In this study, this methodology will be tested to verify that results from conventional methodology could agree with the ones obtained with Taguchi. *Minitab software* is a well-known data analysis tool; it will be used for Taguchi analysis performance.

Taguchi method requires to define some variables: control and noise factors. Control factors are those the research can directly and easily modify (*flowrate, catalytic load and light intensity*), while noise factors are those difficult to control. In this case, the noise factor is not tested but it could be the dispersion of the photocatalytic through the electrode.

Variability is reduced by dampening the effect of noise levels by choosing the proper levels of control factors. To achieve this, Taguchi introduced a statistical parameter called signal-to-noise ratio (S/N), as was previously explained. The signal to noise (S/N) ratio in this study consolidates two repetitions into one value that reflects the amount of variation present.

The higher the S/N, the less variability the system has. As the target variable in this study is to maximize the methanol yield and its Apparent Quantum Efficiency, the signal to noise ratio will correspond to “higher the better” equation. It will be quantified as follows:

$$(S|N_{HB}) = -10\log\left(\frac{1}{r}\cdot\sum_{i=1}^{r}\frac{1}{{y_i}^2}\right) \quad (4)$$

Where:

$r = number\ of\ repetitions$

$y_i = experimental\ value$

4. RESULTS

4.1. Activity with time

Before starting with the optimization of operation variables, the total production rate at the photoactive surfaces was studied at longer experimental times and uses of the material. Total production rate was determined as the amount of carbon species produced from CO_2 during the experiments. Methanol was observed during the first two uses, while traces of isopropanol were detected only during the last experiment. A progressive deactivation of the material is observed during the first use, which goes to the same initial value than in the third use.

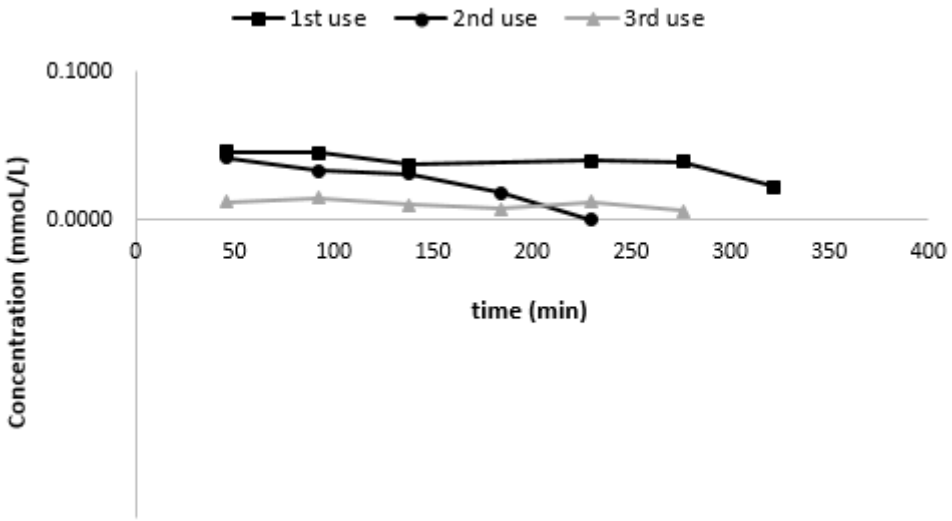

Figure.12 *Catalytic* TiO_2 nanoparticle activity determination. 1mg/cm^2 electrode at 109 µL/min and at 130 W/m^2.

After all the experiments, the color of the catalytic material turns orange; it is an indicator of oxidation phenomena. Based on this observation and ***Fig.12*** results, it is recommended not to use the electrode more than twice. For this reason, for each experiment a photoelectrode with only one use will be tested. Besides, an according to

these data, samples will be taken in a fix time interval of 90 minutes, where pseudo-steady conditions are reached.

4.2 Operation Conditions for TiO_2-based surfaces

A. Effect of the liquid flowrate

Fig.13 compares the performance of the optofluidic microreactor-based system for a liquid flowrate ranging between 85 to 165 µl/min. The load of the electrode and the light intensity were maintained constant during the experimental time (1mg/cm^2 and 85 W/m^2). As it can be seen, 125 µl/min is the flowrate that favored the most methanol productivity and its AQY under set conditions. The maximum productivity was *r*= (5±1) x10^{-7} *MeOH mol/cm^2·h* and the *AQY*=3.31%.

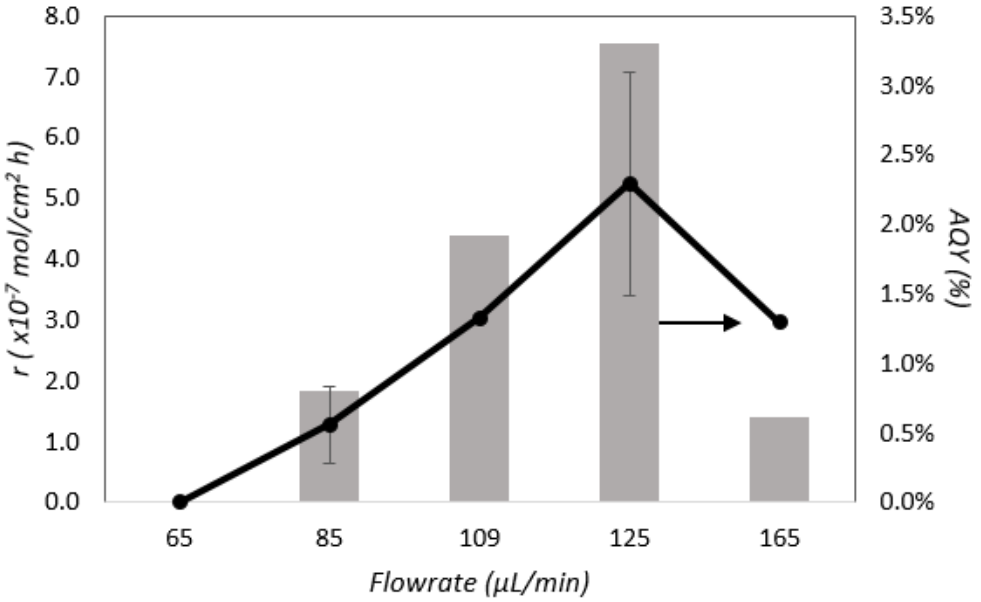

Figure.13 Effect of the liquid flowrate on methanol productivity and AQY for a 1mg/cm^2 electrode at 86 W/m^2

As observed, increases in liquid flowrate result beneficial for CO_2 photoreduction up to 125 µL/min. This may denote an insufficient amount of CO_2 available to react at the semiconductor surface and the possible oxidation of methanol in the microchamber. Further increases in flow rate produce a reduction in both, r and AQY, mainly explained by a decreased in residence time, which may not favour CO_2 conversion, and the liquid pressure increases so that more liquid phase was able to penetrate the carbon paper, hindering CO_2. An intermediate flowrate, 125 µl/min, is adequate for this system, since it provides the best results, r= 5 x10^{-7} MeOH mol/cm^2·h and the AQY=3.31%.

B. Effect of the light intensity

Fig.14 compares the performance of the optofluidic microcell for an irradiance ranging from 85 to 260 W/m^2. The load of the photoelectrode and the flowrate were maintained at 2 mg/cm^2 and 109 µl/min, respectively. In case the distance from the UV- LED to the catalytic surface were 2 cm instead of 5 cm, the irradiance could have been increased up to 1000 W/m^2 (more information is included in Annex).

As it was mentioned in ***METHODOLOGY***, temperature was controlled with an infrared thermometer, so that the temperature of the microreactor almost remained unchanged in all experiments at ambient temperature of 20°C. As it can be seen from ***Fig.14***, higher irradiancies do not enhance optofluidic microreactor performance in terms of r, with almost stable values along the irradiance range. Productivity is r= (2.3±0.8) x10^{-7} *MeOH mol/cm^2· h* and the AQY=0.97% at 129 W/m^2.

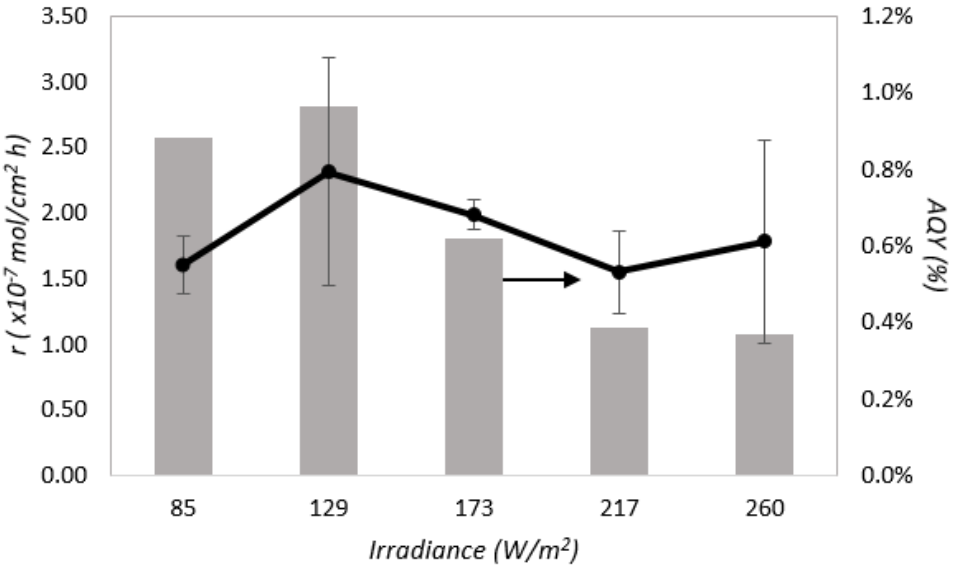

Figure.14 *Effect* of the irradiance on methanol productivity and *AQY* for a 2 mg/cm^2 electrode at 109 µl/min.

As shown in the previous figure, increasing the light intensity involves a decrease in *AQY*. An increase in light intensity can generate more electron-hole pairs for the photocatalytic CO_2 reduction to methanol. However, high irradiancies do not favour methanol productivity either its *AQY*. This phenomenon may be due to secondary reactions that consumes photons and decrease *AQY* for methanol. Analysis of all reaction products remain as a challenge for future work.

C. Effect of TiO_2 loading.

Fig.15 compares the performance of the optofluidic microreactor for a semiconductor loading ranging between 0.5 and 2.5 mg/cm^2. The irradiance and the flowrate were maintained at 85 W/m^{2}and 109 µl/min, respectively. In case of 0.5 mg/cm^2 any methanol was detected but some traces of IPA were observed by GC-FID, thus an experiment without light was run to prove if the IPA come from the CO_2 reduction or from material degradation of the electrode. No IPA was detected in that case, confirming the hypothesis that CO_2 may have been reduced to IPA under light irradiation; although further experimental work is required.

An electrode of 3 mg/cm^2 was also tested, but no methanol was obtained. Based on ***Fig.15*** data, high loading does not promote good results in the system. Best performance is achieved when TiO_2 loading is 1 mg/cm^2. For this case, productivity is *r*= (3.04 ± 0.04) x10^{-7} *MeOH mol/cm^2 ·h* and the *AQY*=1.92 %.

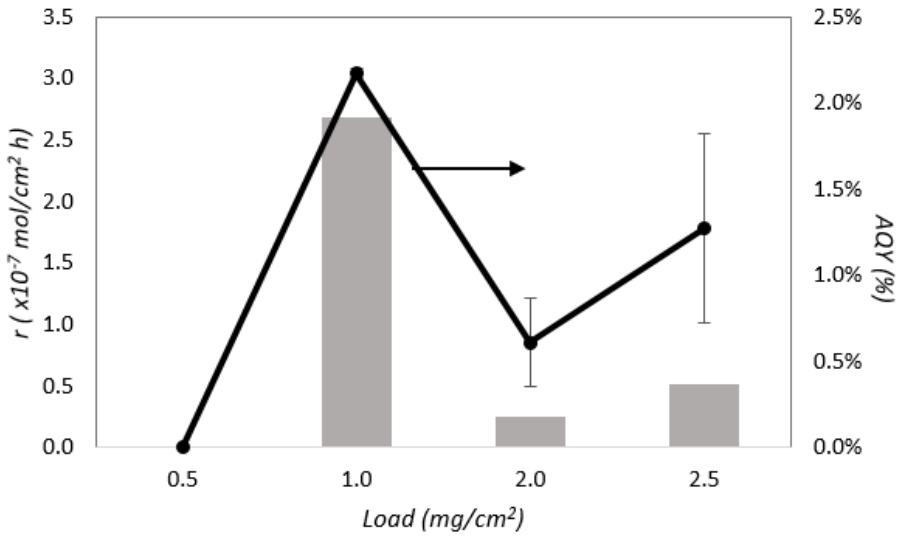

Figure.15 *Effect* of semiconductor loading on methanol productivity and AQY at 86 W/m^2 and a flowrate of 109 µl/min.

Transport resistance and active surface area depends on catalytic thickness, so CO_2 and photons transport can be highly affected with little variations in electrode loading. When the catalyst loading was increased from 1 mg/cm^2 to 2.5 mg/cm^2, both the methanol productivity and *AQY* were declined. This is because the thickness of the semiconductor layer became rather large when the catalyst loading was increased, that it greatly increasing the transfer resistance [20]. Other aspect to be considered is the

agglomeration among TiO_2 nanoparticles that may decrease the available active catalytic area for the reduction of CO_2. Hence, not only the photocatalysts inside of the entire catalytic layer could not be efficiently utilized but also the mass transfer of the CO_2 was resisted seriously. For the 2 mg/cm^2 load catalytic surface, Ion Chromatograph detected some traces of formic acid.

For further studies, a deeper characterization of the shapes/surface areas of the nanoparticles applied should be included to analyze how these variables affect the reaction performance.

4.3 Taguchi and best operation conditions.

One factor experiment evaluates the effect of one parameter on performance while ostensibly holding everything else constant. If there happens to be an interaction of the factor studied with some other factor, then this interaction cannot be observed. Besides this aspect, one factor experiment involves a high number of repetitions, making this performance not so effective.

Orthogonality means that factors can be evaluated independently of one another; the effect of one factor does not bother the estimation of the effect of another factor. It provides a balanced experiment: an equal number of samples under the various treatment conditions. For the study of the CO_2 photoreduction system, a *Three-level orthogonal Array L9 Standard* is selected.

Table.2 Three-Level Orthogonal Array L9 Standard and results.

Trial	Flowrate	Load	Irradiance	$X10^{-8}$ MeOH Productivity	$X10^{-8}$ MeOH Productivity	$X10^{-8}$ Mean	S/N
1	109	0.8	130	29.9	28.4	29.15	29.28
2	109	1.5	170	27.9	23.9	25.90	28.18
3	109	2.2	215	16.1	16.5	16.30	24.24
4	125	0.8	170	58.7	46.8	52.75	34.27
5	125	1.5	215	35.5	27.5	31.50	29.75
6	125	2.2	130	22.9	22.2	22.55	27.05
7	165	0.8	215	19.0	21.8	20.40	26.13
8	165	1.5	130	21.1	25.8	23.45	27.27
9	165	2.2	170	17.9	19.7	18.80	25.45

Fig.16 shows the main effects plot for mean methanol productivity and ***Fig.17*** shows the main effects plot for signal-to-noise-ratio. Taguchi's way of conducting robust design starts by reducing the variability of the system to adjust the mean of the result. Variability is reduced by dampening the effect of noise levels by choosing the proper levels of control factors. Flowrate and loading two factors that affect variability of the system the most, which can be seen in ***Fig.17***. As S/N is always larger the better, levels 125 µl/min and 0.8mg/cm^2 are **chosen** to reduce variability of the system, and the mean will be adjusted using the other factor. In this case, best performance is obtained when irradiancy is 170 W/m^2. This value also meets the requirements of higher the better S/N ratio, it provides the highest result.

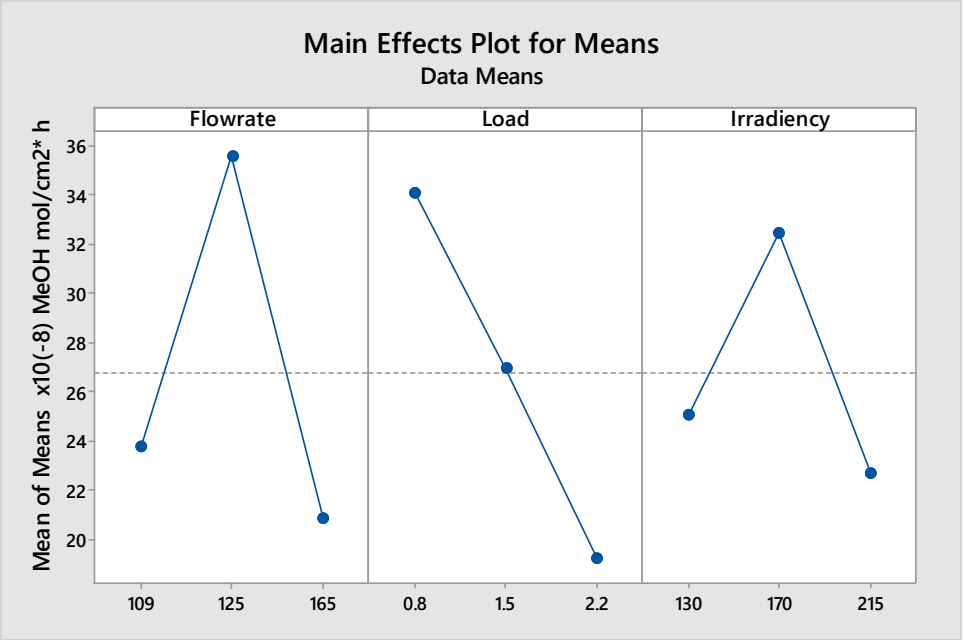

Figure.16 *Main effect plot for methanol productivity means*

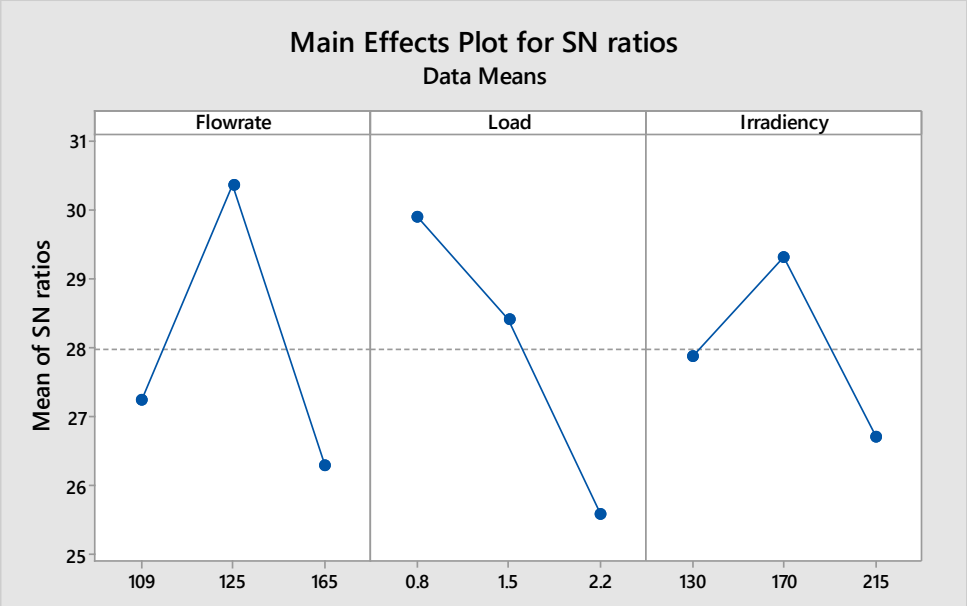

Figure.17 *Main effect plot for Signal-to-Noise ratios.*

Based on Taguchi Methodology best conditions for TiO_2 catalytic electrodes are: 0.8 mg/cm^2, 170 W/m^2 and 125 µl/min. Comparing these values with the ones obtained by the conventional method, the only term that differs is irradiance. According to ***Fig.14,*** there is no a substantial difference between performance at 170 W/m^2 versus at 130 W/m^2. Further work will give more insights into the prediction of CO_2 photoreduction performance by using this methodology.

A semiconductor loading of 1.0 mg/cm^2 was no tested because the interval 0.8 – 1.5 – 2.2 is more balanced and include the range of interest. Taguchi also provides tools for interpolation, so the system performance at a set conditions can be known.

4.4 Comparison of TiO_2 /Cu_2O under UV-light and visible light.

Among various photocatalysts, TiO_2 has attracted much attention owing to its properties, moderate electron transport and appropriate band-edge position. But its wide band gap (3.2 eV) limits the optical response only to UV light (about 5% of total sunlight). ***Fig. 20*** *shows* results of AQY for TIO_2 and Cu_2O/TiO_2 electrode under UV-light and visible light**.** Plot including the results for productivity are not represented because they follow the same tendency as AQY**.** Activity under ultraviolet irradiation is increased 9 times its value (regarding their AQY) when 50/50 Cu_2O/TiO_2 electrode is used. It can be assumed in this case that the role of Cu_2O was not only as a catalyst but also as a hole scavenger and it also promotes the charge separation [30]. One observation to be outlined is that the 50/50 Cu_2O/TiO_2 electrode turned orangish after the first use and it looked as part of the material was peeled off.

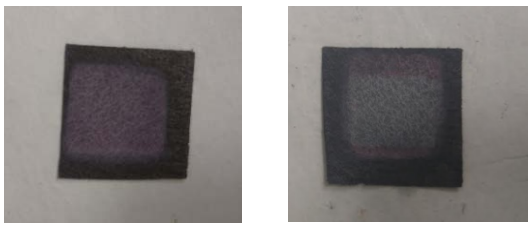

Figure.18 (**a).** Cu_2O/TiO_2 50/50 weight ratio electrode before being used. **(b)** Cu_2O/TiO_2 50/50 weight ratio electrode after the first used. Oxidation phenomena

In order to verify if the electrode was oxidized or some material was removed from the surface, the performance of a new electrode was compared to the orangish electrode. **Fig.19** shows these results. It was verified that performance of the catalytic surface after being used does loss effectiveness.

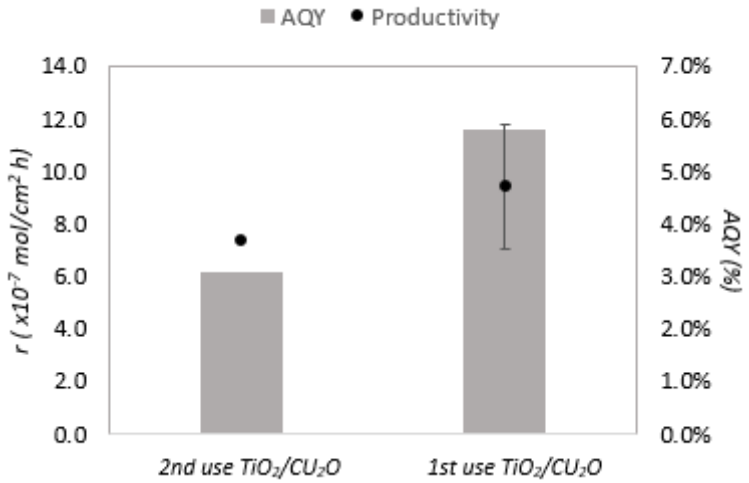

Figure.19. Use effect in Cu_20/TiO_2 50/50 weight ratio electrode

The generally positive effect of Cu_2O on the photocatalytic reaction is ascribed to the ability of the metal to trap electrons and thus reduce recombination losses of the photogenerated charges without affecting the mobility of the electrons [31]. Besides that, Cu_2O bandgap is 2.2 eV and it covers CO_2 reduction and H_2O oxidation reactions potentials. A smaller bandgap does not waste energy in non-interest reactions, such as water reduction. *AQY* to methanol in this case is 9.3%, which is 3 times higher than that value with a TiO_2 photoactive surface.

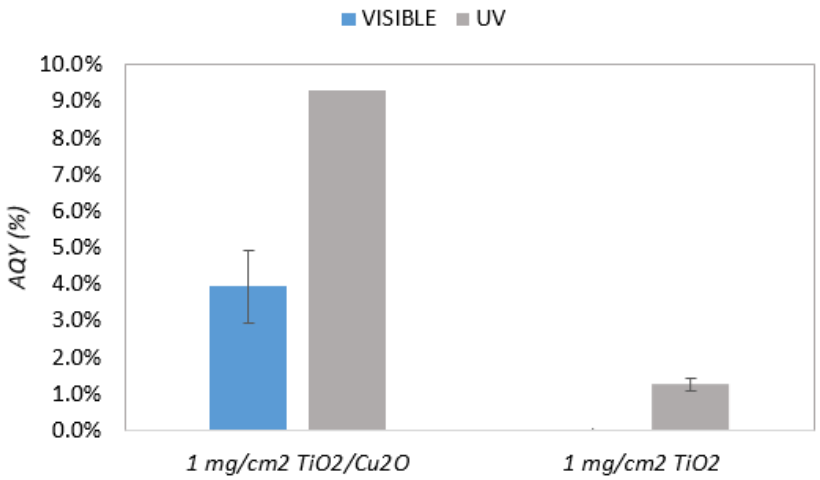

Figure.20. *Effect of Cu_2O addition into the TiO_2 catalytic surface. 50/50 Weight ratio electrode*

Fig.20 also shows data for the best experimental conditions under UV with the TiO_2 surface (125 µl/min, 1mg/cm^2 and at 130 W/m^2); productivity results in r=3.5x10^{-7} *MeOH mol/cm^2 h* and *AQY*=1.46%. However, it should be pointed out that this result does not represent the best performance of the optofluidic microreactor. From ***Fig.13 a***

better result is obtained, productivity is *r*= 5.23x10^{-7} *MeOH mol/cm²·h (AQY=3.31%)* when the system works at 125 µL/min, 1 mg/cm^2 and 85 W/m^2. The only operation variable that is modified regarding ***Fig.20*** is irradiance. According to obtained data in the light intensity effect test, performance at 85 and 130 W/m^2 were very similar, thus, irradiancies within the range of 85 to 130 W/m^2 promote almost the same performance in the system. Taguchi methods also predicted that this variable is the one that less affect variability in the system. Further analysis will be required to better characterize the influence of the irradiance in CO_2 photoreduction.

Cheng et al. also studied TiO_2 in an optofluidic microreactor obtaining a best productivity of 4x10^{-7} MeOH mol/cm^2 ·h. This result is given at the set conditions of: 80W/m^2, a load of 4.5 mg/cm^2 and a flowrate of 25 µL/min. Unless irradiancy, best operation conditions differ from the ones obtained in this study; one of the possible reasons is the ink preparation or slightly differences between microreactors designs.

For the case of visible light, no methanol is detected when only TiO_2 is used. However, when Cu_2O is added into the catalytic surface in a weight ratio of 50/50, CO_2 is reduced into methanol obtaining a better performance than the best result for TiO_2 UV irradiation. The results in this case are *r*= (9.4±0.9) x10^{-7} *MeOH mol/cm²·h (AQY=3.95%).*

5. CONCLUSIONS

In this study, an optofluidic microreactor-based experimental setup has been tested for the continuous photoreduction of CO_2 to methanol. The results may indicate the potential of this reactor designs for an enhancement in transformation of CO_2 to methanol and promoting CCU technologies for a more environmental development. Regarding other designs, such as optical-fiber photo reactor, a significant progress has been shown. Future research should focus on the development and improvement of optofluidic microreactors. Although the optofluidic microreactor has shown some advantages regarding previous designs, there exists still limitations for a practical application. To increase the throughput, an integration of several microreactors in parallel can be introduced.

First material used has been TiO_2 because of its photoreduction properties. The concentration of methanol production after 90 min under the best conditions and UV-

irradiation was *r*= (5±1) x10^{-7} MeOH mol/cm^2 ·h (AQY was 3.31%), while under visible light-irradiation no methanol was detected.

The most significant reason for the low conversion efficiency of TiO_2 under visible light is due to the large value of the band gap (anatase Ebg = 3.2 eV, rutile Ebg = 3.0 eV and brookite Ebg = 3.4 eV) and its high charge recombination rate. One of the possible effects is that the CO_2 reduction only progressed to some reaction intermediate and not to methanol, so the Gas Chromatograph could not detect it.

One of the principal reasons for the better performance when Cu_2O is used is that the band structures of the Cu_2O and TiO_2 match well with each other, in which the conduction band edge of Cu_2O is higher than that of TiO_2, while the valence band edge of TiO_2 is lower than that of Cu_2O. Under UV–visible light irradiation, the electrons on the conduction band of Cu_2O will quickly move to the conduction band of TiO_2, whereas the holes on the valence band of TiO_2 will transfer to the valence band of Cu_2O, effectively realizing the charge separation process. The results are *r*= 2.23x10^{-6} *MeOH mol/cm^2 · h* and *AQY*= 9.29%. Under visible light, *r*= 9.4 x10^{-7} *MeOH mol/cm^2 · h (AQY=3.95%) were obtained.*

Next step involves the use of TiO_2/Cu *core-shell* nanoparticles in the catalytic surface. Because of its morphology and structure, they can improve the system performance. Further investigation and investment is required for the complete development of this technology.

6. CHALLENGES AND PERSPECTIVES

One of the key research lines for this technology lies on the development and characterization of photoactive materials. Besides that, coupling semiconductors with metal nanoparticles and combination of semiconductors, such as Cu_2O/ZnO, have been shown to be beneficial for the performance in CO_2 reduction; facets control and new morphologies development are also very relevant in this field.

Based on previous studies, a further research could be the implementation of biomolecules to the system. The integration of carbon monoxide dehydrogenases (CODHs) could improve the performance of the system since these enzymes catalyze the bioconversion of CO and CO_2. Some authors have previously reported photo assisted

CO_2 reduction using an enzyme-semiconductor complex catalyst, where sunlight was used to harvest a semiconductor. The generating reducing power generated by sunlight was subsequently transferred from the semiconductor to the enzyme for the CO_2 reduction.

Adding biomolecules to the microreactor can involve enzyme detachment from the semiconductor surface. Thus, future approaches in the design should consider these aspects. One recommendation would be the development of the kinetic model for a better understanding of the system, independently if biomolecules were used.

7. REFERENCES

[1] W. Tu, Y. Zhou, and Z. Zou, “Photocatalytic Conversion of CO 2 into Renewable Hydrocarbon Fuels : State-of-the-Art Accomplishment , Challenges , and Prospects,” pp. 4607–4626, 2014.

[2] "Science & Information for a climate-smart nation". [Online]. Available: *https://www.climate.gov*. [Accessed: 29-mar-2018]

[3] " Mauna Loa Observatory, National Oceanic & Atmospheric Administration". [Online]. Available: *www.esrl.noaa.gov/gmd/ccgg/trends/full.html* [Accessed: 29-mar-2018]

[4] S. N. Habisreutinger, L. Schmidt-mende, and J. K. Stolarczyk, “Photocatalytic Reduction of CO 2 on TiO 2 and Other Semiconductors Angewandte,” pp. 7372–7408, 2013.

[5] W. R. Stahel, “Circular economy,” pp. 6–9, 2016.

[6] Climate Change 2013. Summary for political responsabilities and frequent questions. IPPC, 2013.

[7] "Carbon Dioxide Utilization Network". [Online]. Available: *http://co2chem.co.uk/* [Accessed: 31-mar-2018].

[8] J. R. Seth and P. P. Wangikar, “Challenges and opportunities for microalgae-mediated CO 2 capture and biorefinery,” Biotechnol. Bioeng., vol. 112, no. 7, pp. 1281–1296, 2015

[9] S. R. Lingampalli, M. M. Ayyub, and C. N. R. Rao, “Recent Progress in the Photocatalytic Reduction of Carbon Dioxide,” 2017.

[10] J. Albo, M. Alvarez-Guerra, P. Castaño, and A. Irabien, “Towards the electrochemical conversion of carbon dioxide into methanol,” Green Chem., vol. 17, no. 4, pp. 2304–2324, 2015.

[11] M. Pérez-fortes, J. C. Schöneberger, A. Boulamanti, and E. Tzimas, “Methanol synthesis using captured CO 2 as raw material : Techno-economic and environmental assessment,” Appl. Energy, vol. 161, pp. 718–732, 2016.

[12] A. L. Linsebigler, G. Lu, and J. T. Yates, “Photocatalysis on TiO2Surfaces: Principles, Mechanisms, and Selected Results,” *Chem. Rev.*, vol. 95, no. 3, pp. 735–758, 1995.

[13] A. H. Yahaya, M. A. Gondal, and A. Hameed, “Selective laser enhanced photocatalytic conversion of CO2into methanol,” *Chem. Phys. Lett.*, vol. 400, no. 1–3, pp. 206–212, 2004.

[14] Armand Products Company, “Potassium Bicarbonate Handbook,” 2008.

[15] N. Gupta, M. Gattrell, and B. MacDougall, “Calculation for the cathode surface concentrations in the electrochemical reduction of CO2in KHCO3solutions,” *J. Appl. Electrochem.*, vol. 36, no. 2, pp. 161–172, 2006.

[16] K. Li, X. An, K. H. Park, M. Khraisheh, and J. Tang, “A critical review of CO2 photoconversion: Catalysts and reactors,” *Catal. Today*, vol. 224, pp. 3–12, 2014.

[17] J. Ferreira De Brito, A. Alves, D. Silva, A. J. Cavalheiro, M. Valnice, and B. Zanoni, “Evaluation of the Parameters Affecting the Photoelectrocatalytic Reduction of CO 2 to CH 3 OH at Cu/Cu 2 O Electrode,” *Int. J. Electrochem. Sci*, vol. 9, pp. 5961–5973, 2014.

[18] X. Cheng *et al.*, “An optofluidic planar microreactor for photocatalytic reduction of CO2in alkaline environment,” *Energy*, vol. 120, pp. 276–282, 2017.

[19] R. Chen *et al.*, “High-performance optofluidic membrane microreactor with a mesoporous CdS/TiO2/SBA-15@carbon paper composite membrane for the CO2photoreduction,” *Chem. Eng. J.*, vol. 316, pp. 911–918, 2017.

[20] X. Cheng et al., “Optofluidic membrane microreactor for photocatalytic reduction of CO2,” Int. J. Hydrogen Energy, vol. 41, no. 4, pp. 2457–2465, 2016.

[21] J. C. S. Wu and H. Lin, “Photo reduction of CO_2 to methanol via TiO_2 photocatalyst,” Int. J. Photoenergy, vol. 07, pp. 115–20, 2005.

[22] R. Daghrir, P. Drogui, and D. Robert, “Modi fi ed TiO 2 For Environmental Photocatalytic Applications : A Review,” 2013.

[23] O. Ola and M. M. Maroto-valer, “Journal of Photochemistry and Photobiology C : Photochemistry Reviews Review of material design and reactor engineering on TiO 2 photocatalysis for CO 2 reduction,” "Journal Photochem. Photobiol. C

Photochem. Rev., vol. 24, pp. 16–42, 2015.

[24] Handoko, A. D. and Tang, J. (2013) “Controllable proton and CO 2photoreduction over Cu 2 O with various morphologies,” *International Journal of Hydrogen Energy*, 8, pp. 1–6. doi: 10.1016/j.ijhydene.2013.03.128.

[25] J. Wang, G. Ji, Y. Liu, M. A. Gondal, and X. Chang, “Cu2O/TiO2heterostructure nanotube arrays prepared by an electrodeposition method exhibiting enhanced photocatalytic activity for CO2reduction to methanol,” *Catal. Commun.*, vol. 46, pp. 17–21, 2014.

[26] L. Jia, J. Li, and W. Fang, “Enhanced visible-light active C and Fe co-doped LaCoO 3 for reduction of carbon dioxide,” *Catal. Commun.*, vol. 11, no. 2, pp. 87–90, 2009.

[27] K. G. Rao, “Green Synthesis of TiO 2 Nanoparticles Using Hibiscus Flower Extract,” no. May, 2016.

[28] J. Albo, A. Sáez, J. Solla-Gullón, V. Montiel, and A. Irabien, “Production of methanol from CO<inf>2</inf> electroreduction at Cu<inf>2</inf>O and Cu<inf>2</inf>O/ZnO-based electrodes in aqueous solution,” *Appl. Catal. B Environ.*, vol. 176–177, pp. 709–717, 2015.

[29] Phillip J. Ross. “Taguchi techniques for quality Engineering”. New York, NY, USA. McGraw-Hill, 2nd Edition. 1996.

[30] Xu, H. et al. (2014) “Porous-structured Cu_2O/TiO_2 nanojunction material toward efficient CO2 photoreduction,” Nanotechnology, 25(16). doi: 10.1088/0957-4484/25/16/165402.

[31] Handoko, A. D. and Tang, J. (2013) “Controllable proton and CO_2 photoreduction over Cu_2O with various morphologies,” International Journal of Hydrogen Energy, 8, pp. 1–6. doi: 10.1016/j.ijhydene.2013.03.128.

8. ANNEX

8.1 Characterization of the pilot plant set up

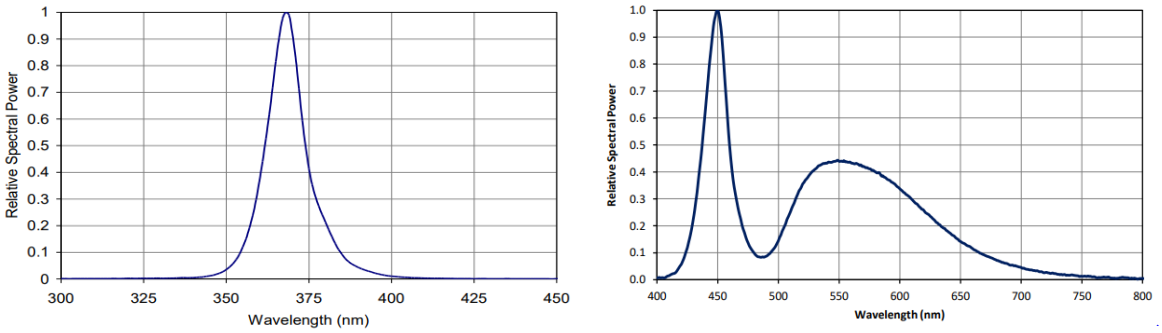

(a) *(b)*

Figure A1. Typical relative spectral power vs. wavelength at 25°C. **(a)** 365nm UV LED Gen2 Emitter LED ENTER. **(b)** High Luminous Efficacy Cool White LED Emitter LED ENTER.

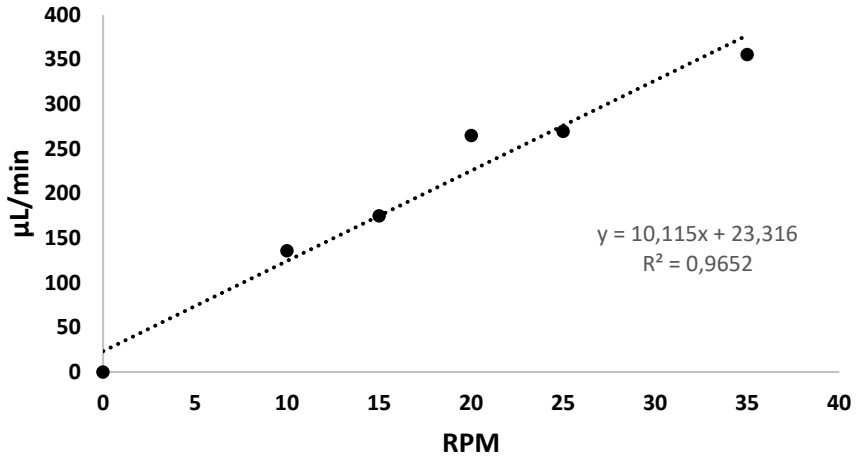

Figure A2. Calibration curve for inlet flowrate controlled by Peristaltic Pump Miniplus 3 Gilson

8.2 LED Characterization regarding distance to the catalytic surface

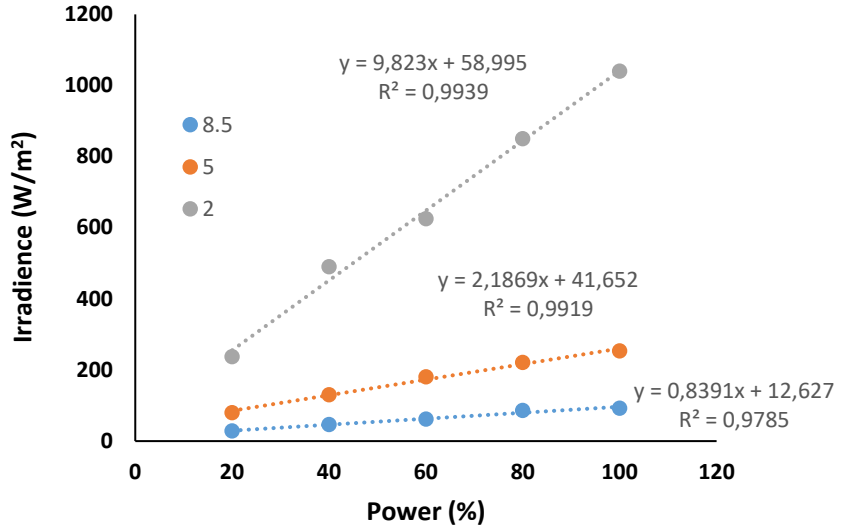

Figure A3. Irradiance of UV LED at difference distance from the electrode surface: 2; 5 and 8.5cm.

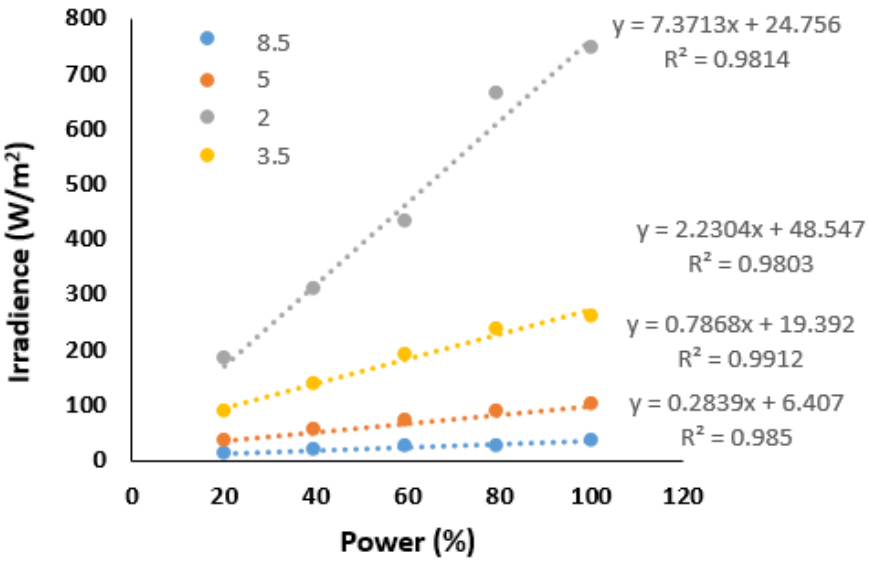

Figure A4. Irradiance of visible light LED at difference distance from the electrode surface: 2; 3.5; 5 and 8.5cm.

8.3 Calibration lines for the studied compounds.

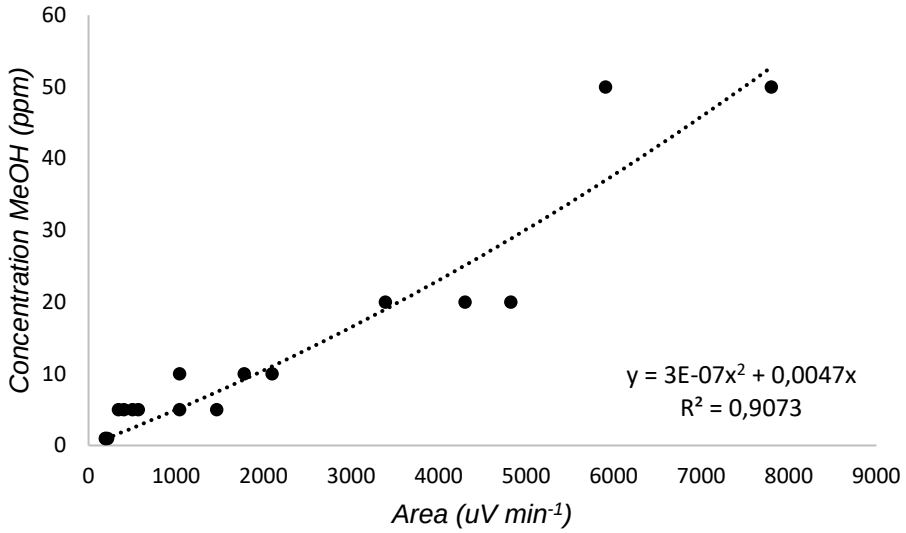

Figure A5. Calibration curve for methanol concentration detected by Gas chromatograph (GCMS-QP2010 Ultra Shimadzu)

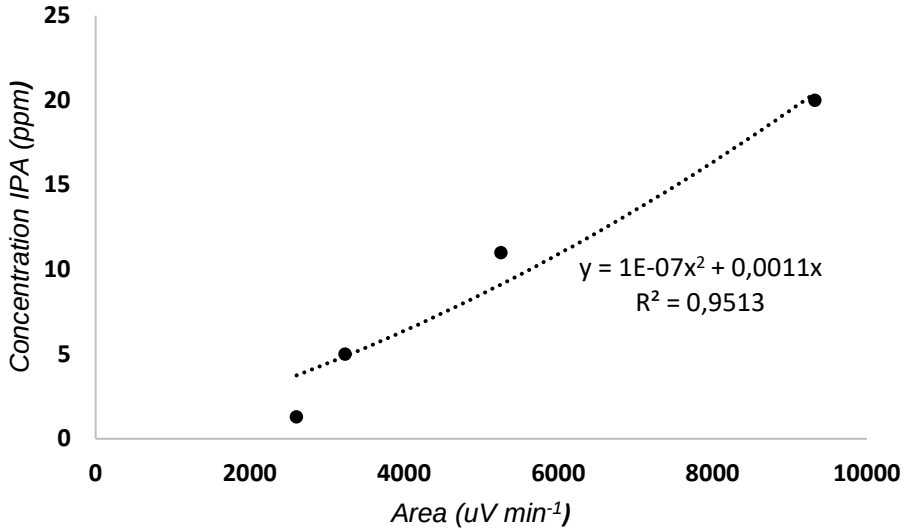

Figure A6. Calibration curve for isopropanol concentration detected by Gas chromatograph (GCMS-QP2010 Ultra Shimadzu)

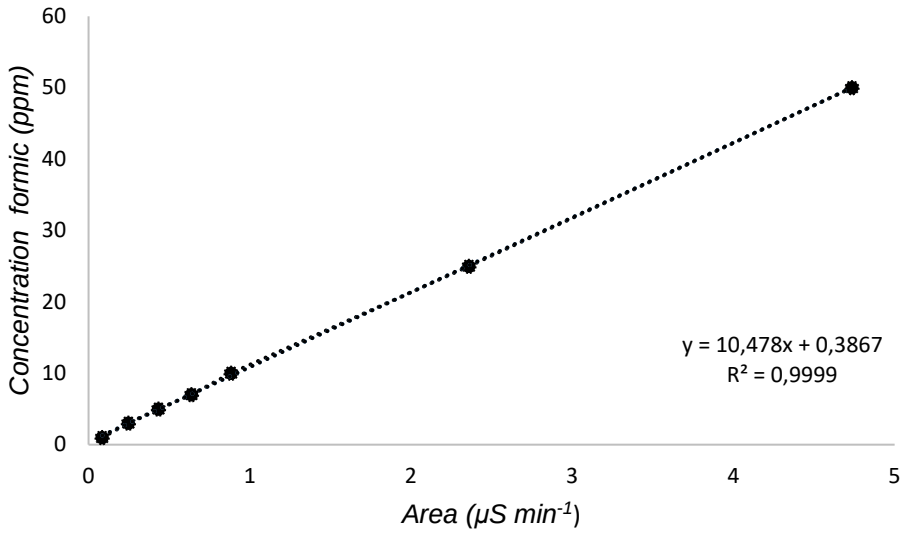

Figure A7. Calibration curve for formic acid concentration detected by Ion Chromatography (IC)